ELSEVIER

Thermochimica Acta 244 (1994) 205–221

thermochimica acta

Thermal and Mössbauer studies of iron-containing hydrous silicates. Part 8. Chrysotile

K.J.D. MacKenzie *, D.G. McGavin

New Zealand Institute for Industrial Research and Development, P.O. Box 31-310, Lower Hutt, New Zealand

Received 20 October 1993; accepted 28 January 1994

Abstract

The thermal analysis, X-ray powder diffractometry and ^{57}Fe Mössbauer spectroscopy of a New Zealand chrysotile indicate that heating in air produces a fully ferric chrysotile before the onset of dehydroxylation at about 600°C. During the low-temperature oxidation of octahedral Fe^{2+}, tetrahedral Fe^{3+} also moves into vacant octahedral sites. On heating in air above 700°C, forsterite (Mg_2SiO_4) is formed, followed, above 800°C, by enstatite ($MgSiO_3$), these phases forming via two different dehydroxylates. During heating in air at 900–1300°C, up to 70% of the Fe^{3+} progressively reverts to Fe^{2+}, the Mössbauer parameters of which correspond more with those of enstatite than of forsterite. A possible mechanism for this unexpected iron behaviour is discussed, in terms of cation vacancies. Some practical implications of these results on the thermal destruction of chrysotile toxicity and on the geochemistry of pyroxene formation from serpentines are also noted.

Keywords: Chrysotile; DTA; DTG; EDAX; Mechanism; Mössbauer; Silicate; Toxicity; XRPD

1. Introduction

Chrysotile, or white asbestos, is the fibrous form of serpentine, the 1:1 trioctahedral layer lattice magnesiosilicate of ideal composition $Mg_3Si_2O_5(OH)_4$. For many

* Corresponding author.

SSDI 0040-6031(94)01795-I

years, chrysotile was used extensively in many building applications, as a non-flammable insulating material, and as an engineering friction material in brakes and clutches. However, over the last decade, the use of chrysotile and other asbestiform minerals has decreased markedly as the health risks associated with the respiration of fibrous materials have become better understood. This in turn has led to increased research interest in methods for converting chrysotile into less harmful products, while retaining its most desirable physical properties. Because a number of these procedures involve a thermal degradation step, the thermal decomposition sequence of chrysotile has recently been re-examined using a variety of techniques, including solid-state nuclear magnetic resonance spectroscopy [1], which suggests that the dehydroxylation of chrysotile and its conversion into forsterite (Mg_2SiO_4) and enstatite ($MgSiO_3$) is more complex than previously thought.

Structurally, serpentine is the magnesian analogue of kaolinite, consisting of alternate sheets of Si–O tetrahedra and Mg–O(OH) octahedra, but differing from kaolinite in their mode of layer stacking. There are three distinguishable serpentine polymorphs: lizardite, which assumes a block-like morphology; antigorite, in which the misfit between the tetrahedral and octahedral sheets is relieved by corrugating of the layers; and chrysotile, in which the sheets are rolled into fibres about the x-axis. Although the presence of iron is not a requirement of the ideal structure, it usually occurs in chrysotiles to the extent of several percent, up to about a third of which is in the Fe^{2+} form, substituting for octahedral Mg^{2+}, and two-thirds in the Fe^{3+} form, substituting for both Mg and Si [2]. A brief Mössbauer study of lizardite heated in helium up to 850°C has been reported in the context of an investigation of carbonaceous chondritic meteorites [3], but the behaviour of the iron in chrysotile during the thermal reaction sequence in air is unknown. The aim of the present work is to provide this information, to complement the recently available ^{29}Si and ^{25}Mg NMR results which suggest the formation of two intermediate dehydroxylates which have different structures, thermal stabilities and reaction paths [1].

2. Experimental

The chrysotile used in this study was from the Upper Takaka Valley asbestos deposit, NW Nelson, New Zealand. X-ray diffractometry showed this to be clinochrysotile, similar to JCPDS card no. 31-808, with no contaminating mineral phases such as are sometimes present in chrysotile, e.g. brucite [4,5], magnesite [5] and magnetite [2]. Elemental analysis by EDAX showed that the only detectable element other than Si and Mg is Fe, present at a level of 1.16%. Thermal analysis was carried out in air at a heating rate of 10°C min^{-1} using a Stanton-Redcroft TG770 thermobalance and a Perkin-Elmer DTA 1700 differential thermal analyser. Samples for Mössbauer spectroscopy were sequentially heated in air in a platinum crucible for 15 min at each temperature. After heating, the sample was examined by X-ray powder diffractometry (Philips PW 1700 computer-controlled diffractometer with Co Kα radiation and graphite monochromator), and by Mössbauer spectroscopy, before being re-heated to the next temperature.

The Mössbauer spectra were obtained in transmission mode at room temperature using a constant acceleration spectrometer with a 10 mCi source of ^{57}Co in Rh. Data were transferred to a computer using EG&G Ortec multichannel scaling hardware and software. The spectra were computer-fitted using a non-linear least-squares program. Metallic iron was used to calibrate the velocity scale and as a reference for the isomer shifts.

3. Results and discussion

3.1. Thermal analysis of Nelson chrysotile

The thermal analysis traces of Nelson chrysotile are shown in Fig. 1. The thermal traces are typical of those reported by Khorami et al. [5] for extremely pure

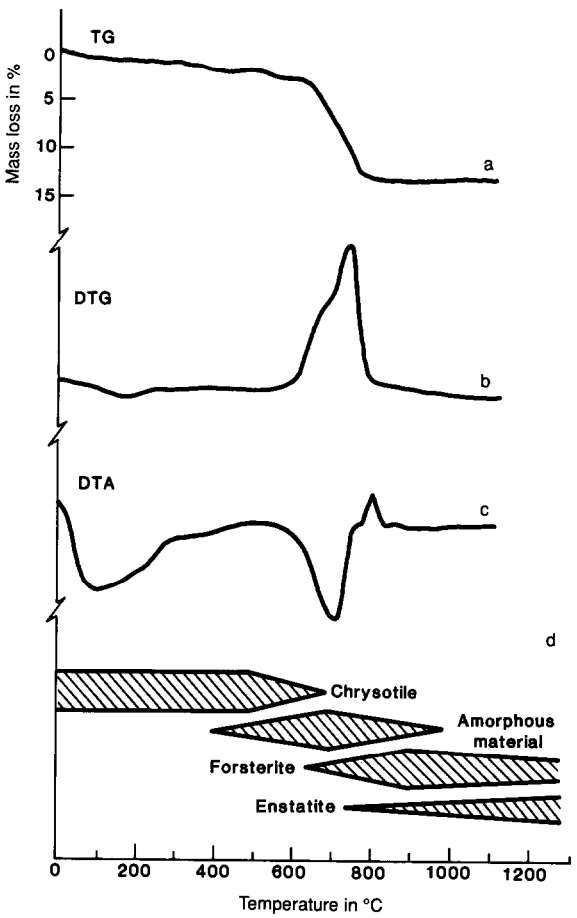

Fig. 1. Curves a–c, thermal analysis traces of Nelson chrysotile, heating rate 10°C min^{-1} in air. Section d, schematic representation of the corresponding phase changes, determined at room temperature by X-ray powder diffractometry.

chrysotile, in which the endothermic weight loss at about 100°C corresponds with the loss of water adsorbed on to the fibre surfaces. The major endothermic weight loss at about 700°C corresponds with the loss of structural hydroxyl water. The shoulder seen at about 630°C, especially in the DTG trace (Fig. 1, curve b) was also reported by Khorami et al. [5], who used evolved gas analysis (EGA) to demonstrate that it is associated with chrysotile dehydroxylation, and is not an artifact arising from the decomposition of impurities. A similar effect has also been observed in both the DTG and DTA traces of a Canadian chrysotile [1]. The X-ray powder diffractometry results, which are summarized schematically in Fig. 1, section d, indicate that the onset of the dehydroxylation peak is accompanied by a progressive loss in intensity of the chrysotile reflections, and an increase in the proportion of X-ray-amorphous material, evidenced by the growth of a broad hump in the baseline between about 20 and 45°2θ. The first X-ray indication of the product phase (forsterite) occurs at about the temperature of the main dehydroxylation weight loss (700°C). The forsterite reflections grow in intensity at the expense of the amorphous baseline hump, as the heating progresses. The exotherm at about 810°C (Fig. 1, curve c) has been variously ascribed to the formation of forsterite [6], the recrystallization of disordered forsterite [7], the formation of forsterite and enstatite [8], or more vaguely, "the conversion of chrysotile anhydride" [9]. A recent solid-state NMR study [1] suggests that this exotherm may be associated with the collapse of the oxygen layers of a layer-lattice-type dehydroxylate to form enstatite, which also makes its first X-ray appearance at about this temperature (Fig. 1, section d). Although no further thermal events occur, up to 1000°C, X-ray diffractometry and solid-state NMR indicate further reaction at about 1150°C of forsterite with the amorphous silica present, forming additional enstatite.

3.2. Mössbauer spectroscopy of unheated and heated chrysotile

The room-temperature Mössbauer spectrum of unheated Nelson chrysotile is shown in Fig. 2. This spectrum is similar to those previously reported by Rozenson et al. [10] (who included a Nelson chrysotile in their suite of samples), and also to the spectra of Canadian chrysotiles reported by Blaauw et al. [2] and by O'Hanley and Dyar [11]. A very similar Mössbauer spectrum was also reported for lizardite by Malysheva et al. [3]. The spectrum is well fitted by three quadrupole doublets; the widest, containing 31% of the intensity, has typically ferrous parameters, with an isomer shift (IS) of 1.15 mm s^{-1} and a quadrupole splitting (QS) of 2.72 mm s^{-1}. These parameters are in good agreement with those found for the ferrous site by Rozenson et al. (IS = 1.14, QS = 2.74 mm s^{-1} [10]), Blaauw et al. (IS = 1.12, QS = 2.65 mm s^{-1} [2]), O'Hanley and Dyar (IS = 1.13, QS = 2.71 mm s^{-1} [11]) and Malysheva et al. (IS = 1.18, QS = 2.75 mm s^{-1} [3]). These four groups of authors identify this ferrous site as octahedral, with Rozenson et al. [10] further assigning it as an M2 site, which they suggest is more distorted than the M1 site. However, crystallographic evidence for two distinguishable octahedral sites is so far lacking; the only complete structure determinations available are of three lizardites, in which only one octahedral site is described [12,13].

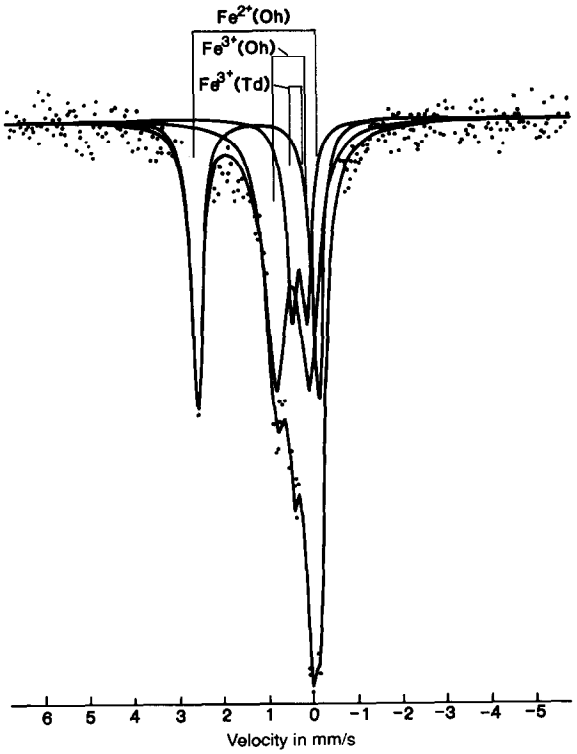

Fig. 2. Room-temperature Mössbauer spectrum of unheated Nelson chrysotile.

The other two doublets have typically ferric Mössbauer parameters. The more intense, which contains 50% of the total iron, has the parameters IS = 0.36, QS = 0.75 mm s^{-1}, comparable with the octahedral ferric doublet of Blaauw et al. (IS = 0.34, QS = 0.75 mm s^{-1} [2]), O'Hanley and Dyar (IS = 0.33–0.35, QS = 0.75 mm s^{-1} [11]) and Malysheva et al. (IS = 0.38, QS = 0.79 mm s^{-1} [3]). These parameters are not, however, in agreement with those found by Rozenson et al. [10] for their octahedral ferric doublet (IS = 0.38, QS = 1.08 mm s^{-1}); it is not clear why their QS value for this site, which they identify as the more distorted M2 site, should be significantly larger than those found by other workers.

The second ferric doublet, containing 19% of the total iron, has typically tetrahedral parameters (IS = 0.19, QS = 0.34 mm s^{-1}), in reasonable agreement with the tetrahedral values of Blaauw et al. (IS = 0.2, QS = 0.34 mm s^{-1} [2]), Malysheva et al. (IS = 0.24, QS = 0.32 mm s^{-1} [3]), O'Hanley and Dyar (IS = 0.17–0.18, QS = 0.33–0.35 mm s^{-1} [11]) and Rozenson et al. (IS = 0.27, QS = 0.30 mm s^{-1} [10]). Although the latter workers are hesitant to assign this site to tetrahedral Fe^{3+} because its isomer shift is larger than they would have expected for a tetrahedral site, they note that doublets of similar parameters in the 2:1 layer silicate nontronite have been identified as tetrahedral [10].

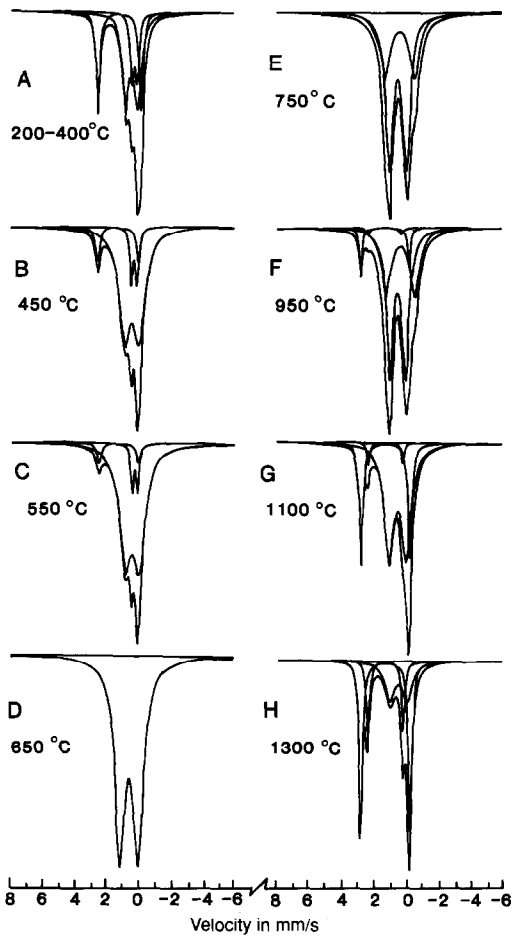

Fig. 3. Room-temperature Mössbauer spectra of Nelson chrysotile, heated in air for 15 min to the indicated temperatures.

Typical room-temperature Mössbauer spectra of Nelson chrysotile heated to various temperatures are shown in Fig. 3, and the corresponding Mössbauer parameters are listed in Table 1. Heating the chrysotile in air below 200°C produces little change in the Mössbauer spectrum, but above 200°C, the onset of oxidation is marked by a decrease in the area of the Fe^{2+} doublet, with a corresponding increase in octahedral Fe^{3+}. The tetrahedral Fe^{3+} doublet also begins to decrease over this temperature interval. The change in the relative site occupation with temperature is shown in Fig. 4 which indicates that the major decrease in the area of the Fe^{2+} doublet occurs between 300 and 500°C, with a concomitant reduction in the tetrahedral Fe^{3+} site occupancy to about half its original value. This doublet disappears completely from the spectrum between 600 and 650°C, at which temperature the Fe^{2+} has also been completely oxidised. The total iron content of this

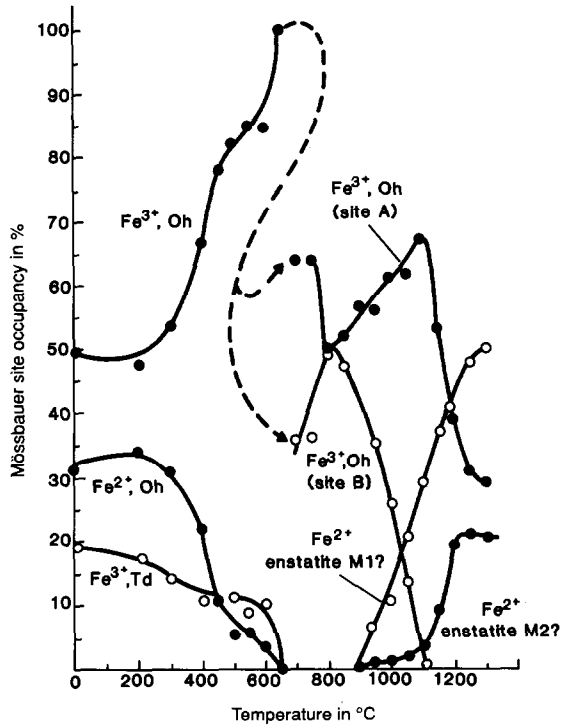

Fig. 4. Changes in occupancy of the various iron sites with heating temperature: Oh, octahedral sites; Td, tetrahedral sites. Solid lines showing trends in these parameters take account of the experimental uncertainties in the data.

sample occurs in an octahedral doublet, the components of which have, however, achieved their maximum linewidth (0.90 mm s^{-1}). This is also the temperature at which the chrysotile XRD reflections have disappeared and the X-ray-amorphous dehydroxylate phase is present in maximum concentration, as judged by the broad hump in the XRD baseline.

By 700°C, the single broad Fe^{3+} resonance can be fitted better by two ferric doublets, one of which, designated site A, has Mössbauer parameters which are not too dissimilar to those of the original octahedral Fe^{3+} site (a more detailed discussion of the Mössbauer parameters follows below). The new site, designated site B, is probably ferric, although its IS is considerably smaller and its QS significantly larger than those of site A. On heating to higher temperatures, the population of site A increases slightly, but that of site B decreases markedly between 900 and 1050°C, this decrease being partly accounted for by the appearance and growth of new Fe^{2+} doublets at 950°C and 1100°C (Fig. 4).

Figs. 5 and 6 show the changes in the Mössbauer parameters of the Fe^{3+} and Fe^{2+} doublets respectively, as a function of heating temperature. Figs. 5 and 6 show that the parameters of all the initial doublets are not greatly changed by heating

Table 1
Mössbauer parameters for unheated and heated Nelson chrysotile in mm s^{-1}; uncertainties in values are indicated in parentheses; isomer shift values are relative to natural iron

Temperature/°C	Fe^{3+} (octahedral)				Fe^{3+} (tetrahedral)			
	QS	IS	Width	Occupancy/%	QS	IS	Width	Occupancy/%
RT	0.75(4)	0.36(2)	0.54(4)	50(3)	0.34(4)	0.19(2)	0.29(5)	19(3)
200	0.79(7)	0.36(3)	0.57(8)	48(4)	0.32(4)	0.20(2)	0.25(7)	18(4)
300	0.79(6)	0.35(3)	0.61(6)	54(4)	0.32(3)	0.19(2)	0.23(6)	15(4)
400	0.87(5)	0.35(3)	0.81(6)	67(3)	0.33(3)	0.17(2)	0.21(5)	11(3)
450	0.91(4)	0.33(1)	0.87(3)	78(2)	0.36(2)	0.18(1)	0.23(4)	11(2)
500	0.90(4)	0.33(1)	0.86(4)	82(2)	0.36(7)	0.18(3)	0.25(4)	12(2)
550	0.89(4)	0.33(2)	0.90(4)	85(3)	0.35(4)	0.17(2)	0.21(5)	9(2)
600	0.99(5)	0.34(2)	0.90(5)	84(3)	0.39(4)	0.18(2)	0.22(4)	11(2)
650	1.16(1)	0.34(1)	0.79(1)	100				
700	1.04(2)	0.35(1)	0.57(3)	64(4)				
750	1.05(2)	0.35(1)	0.56(3)	64(4)				
800	1.04(2)	0.36(1)	0.54(3)	50(3)				
850	1.03(2)	0.36(1)	0.53(3)	52(3)				
900	1.02(2)	0.36(1)	0.54(3)	57(4)				
950	0.98(2)	0.36(1)	0.52(3)	56(4)				
1000	0.98(2)	0.36(1)	0.57(3)	61(3)				
1050	0.98(2)	0.36(1)	0.61(3)	62(2)				
1100	1.08(2)	0.37(1)	0.72(3)	67(1)				
1150	1.07(3)	0.35(1)	0.71(4)	53(2)				
1200	1.06(3)	0.35(2)	0.65(5)	40(2)				
1250	1.04(5)	0.36(3)	0.64(7)	31(2)				
1300	1.07(6)	0.35(3)	0.72(9)	30(2)				

Fe^{3+} (octahedral)			
QS	IS	Width	Occupancy/%
1.75(7)	0.24(2)	0.75(7)	36(4)
1.83(6)	0.23(2)	0.74(7)	36(4)
1.72(4)	0.17(1)	0.80(4)	50(3)
1.75(4)	0.17(1)	0.77(5)	48(3)
1.82(6)	0.17(2)	0.75(7)	41(4)
1.80(6)	0.19(2)	0.73(7)	36(4)
1.86(7)	0.16(2)	0.68(8)	26(4)
1.94(9)	0.18(3)	0.60(12)	15(2)

Temperature/°C	Fe^{2+} (octahedral)							
	QS	IS	Width	Occupancy/%				
RT	2.72(1)	1.15(1)	0.30(2)	31(2)				
200	2.72(2)	1.15(1)	0.30(3)	34(4)				
300	2.72(2)	1.14(1)	0.26(2)	31(3)				
400	2.67(3)	1.14(1)	0.30(3)	22(2)				
450	2.58(4)	1.19(2)	0.33(6)	11(1)				
500	2.44(14)	1.21(8)	0.36(13)	6(2)				
550	2.48(16)	1.19(8)	0.37(16)	6(2)				
600	2.48(16)	1.20(13)	0.39(23)	4(2)				
650								
700	Fe^{2+} (M1 enstatite?)				Fe^{2+} (M2 enstatite?)			
750								
800	QS	IS	Width	Occupancy/%	QS	IS	Width	Occupancy/%
850								
900	3.05(7)	1.10(3)	0.16(9)	2(1)				
950	3.01(3)	1.13(1)	0.22(4)	7(1)	2.10(15)	1.16(7)	0.25(25)	1(1)
1000	3.05(3)	1.13(1)	0.27(4)	11(1)	2.11(10)	1.15(5)	0.22(17)	2(1)
1050	3.04(1)	1.13(1)	0.27(2)	21(1)	2.05(5)	1.17(2)	0.16(8)	2(1)
1100	3.02(1)	1.14(04)	0.29(2)	29(1)	2.15(5)	1.16(2)	0.21(8)	4(1)
1150	3.01(1)	1.14(04)	0.28(1)	37(2)	2.14(4)	1.13(2)	0.29(6)	10(2)
1200	3.01(1)	1.14(04)	0.27(1)	41(2)	2.15(2)	1.15(1)	0.29(3)	19(2)
1250	3.02(1)	1.14(04)	0.28(1)	48(2)	2.17(2)	1.15(1)	0.29(4)	21(2)
1300	3.02(1)	1.15(04)	0.26(1)	50(2)	2.18(2)	1.15(1)	0.25(3)	20(2)

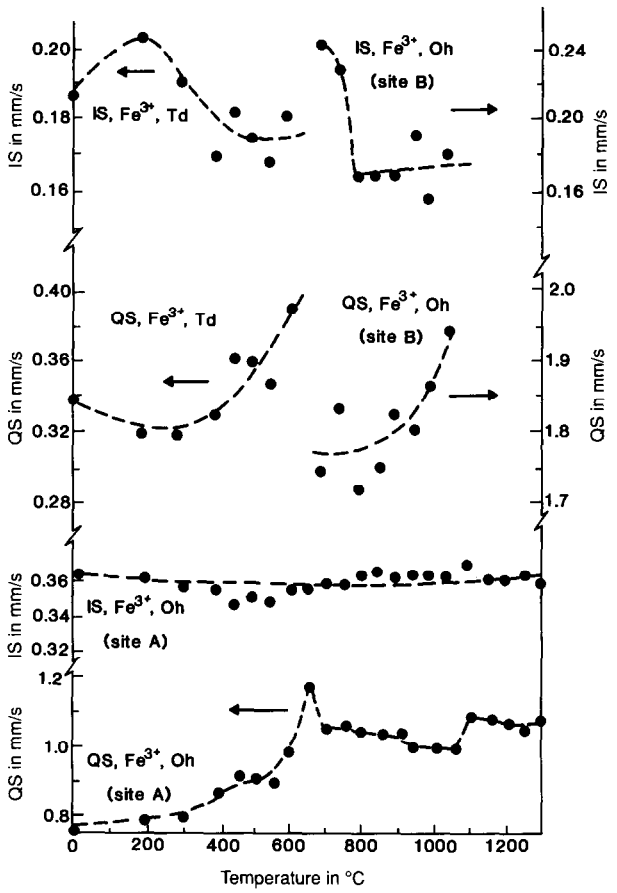

Fig. 5. Changes in the ferric Mössbauer parameters of chrysotile with heating temperature: Oh, octahedral sites; Td, tetrahedral sites. Trend lines take account of the experimental uncertainties in the data. Isomer shifts quoted with respect to natural iron.

below 400°C. Between 400 and 500°C, corresponding to the formation of chrysotile containing largely Fe^{3+}, and the onset of dehydroxylation, the IS value of the tetrahedral Fe^{3+} doublet does not change significantly (Fig. 5), but a greater effect is seen in the IS of the Fe^{2+} doublet, which increases significantly (Fig. 6). The complete dehydroxylation of ferric chrysotile between 500 and 700°C is marked by increases in the QS values of the Fe^{3+} doublets, although their IS values remain relatively static. Following the reasoning of Rozenson et al. [10], more distorted Fe^{3+} sites have larger QS values, the reverse being true for Fe^{2+}. Thus, the behaviour of the QS values on heating is consistent with an increase in distortion of both the ferric and ferrous sites, the effect being more marked during the oxidation of Fe^{2+}, and again during dehydroxylation (Figs. 5 and 6).

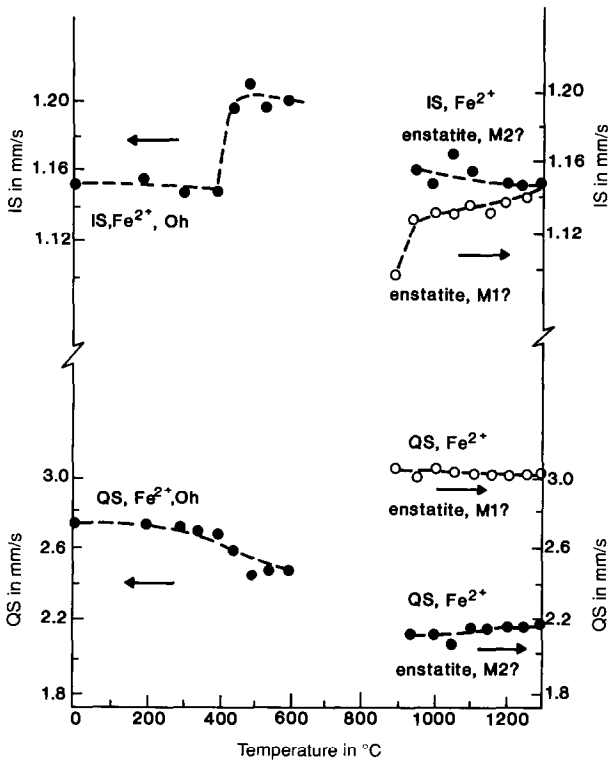

Fig. 6. Changes in the ferrous Mössbauer parameters of chrysotile with heating temperature: Oh, octahedral sites. Trend lines take account of the experimental uncertainties in the data. Isomer shifts quoted with respect to natural iron.

From 700°C, corresponding to the complete disappearance of the chrysotile reflections, two types of Fe^{3+} sites can be resolved. Comparison of the parameters of site A (QS = 0.98–1.08 mm s^{-1}, IS = 0.35–0.37 mm s^{-1}) and site B (QS = 1.72–1.94 mm s^{-1}, IS = 0.16–0.24 mm s^{-1}) with those found for other 1:1 layer lattice silicates heated in air [14] indicates that similar Mössbauer behaviour is shown only by ferric berthierine. The dehydroxylate of this phase contains two Fe^{3+} sites, QS = 1.01–1.06, IS = 0.33–0.36 mm s^{-1}, and QS = 1.5–1.75, IS = 0.31–0.36 mm s^{-1}, the former site being the octahedral ferric site originally present, and the latter a highly distorted octahedral ferric site resulting from the oxidation of Fe^{2+} [15]. From a compositional point of view, both berthierine and amesite are related to serpentine, the former by replacement of all of the Mg by Fe and Al; in the latter, this substitution is only partial. On this basis, greater similarity to the behaviour of amesite than to berthierine might have been expected. It should be noted, however, that the present Mössbauer parameters are not unique to 1:1 layer silicates; indeed, they are more common in the Mössbauer spectra of dehydroxylated 2:1 minerals such as glauconite [16], muscovite [17] and montmorillonite [18], in which the more

highly distorted site of higher QS has been tentatively identified with the 5-coordinate (originally cis) sites which can occur in dehydroxylated 2:1 layer lattice minerals.

On heating above 800°C, the more distorted site B is progressively lost, being replaced in part by a new doublet with parameters typical of Fe^{2+} (IS = 1.10–1.15, QS = 3.01–3.05 mm s^{-1}) (Fig. 6). Shortly after the appearance of this new Fe^{2+} doublet, a second but weaker Fe^{2+} doublet can be resolved, having the parameters IS = 1.13–1.17, QS = 2.05–2.18 mm s^{-1}. The first crystalline reaction product to be formed (forsterite) appears just above 700°C, followed by enstatite at about 800°C (Fig. 1). Although the iron content of both naturally occurring forsterite and enstatite is predominantly ferrous, with preference being shown for the smaller M1 site in forsterite [19] and the M2 site in enstatite [20], small amounts of Fe^{3+} have been found in the Mössbauer spectra of these phases. However, the reported Fe^{3+} parameters in olivine (IS = 0.04, QS = 0.82 mm s^{-1} [19]) are very different from those found in the present samples heated at 700–950°C, suggesting that the bulk of the ferric iron may be located in another phase, possibly the layer-lattice-type dehydroxylate II identified by solid-state MAS NMR in chrysotile heated to this temperature [1]. The appearance of the first of the new ferrous doublets approximately coincides with the temperature at which dehydroxylate II decomposes to form enstatite, and, further, the present parameters are similar to those of Fe^{2+} in the M1 sites of enstatite (IS = 1.21–1.31, QS = 2.95–3.39 mm s^{-1} [21], IS = 1.18–1.306, QS = 2.496–3.131 mm s^{-1} [20]). The Mössbauer parameters of the weaker Fe^{2+} doublet which develops only after further heating coincide reasonably well with those of the M2 site in enstatite (IS = 1.19–1.32, QS = 2.18–2.27 mm s^{-1} [21], IS = 1.139–1.276, QS = 1.971–2.047 mm s^{-1} [20]), but these parameters are also similar to those of forsterite (IS = 0.93, QS = 2.25 mm s^{-1} for M1, IS = 1.00, QS = 2.55 mm s^{-1} for M2 [19]). Thus, the ferrous doublets which develop at the expense of ferric site B could be identified with the M1 and M2 sites of enstatite; although the association of the weaker Fe^{2+} doublet with forsterite cannot be entirely ruled out on the basis of the Mössbauer results, mechanistic considerations (see below) make this less likely.

3.3. The high-temperature ferrous spectrum

Because the observation of the ferrous doublets which unexpectedly develop late in the reaction is unprecedented in the literature on the thermal decomposition of iron-containing silicates, various alternative explanations were investigated.

The possibility that the spectra are an artifact of the spectroscopic technique was ruled out by collecting all the data at a wide velocity setting of ± 10 mm s^{-1}. These results established that the doublets in question are not the inner portion of a magnetic spectrum; neither do their parameters coincide with the unusual Fe^{IV} state, which has a similar QS but a much smaller IS [22].

The possibility that the spectra are an artifact of the sample was investigated by repeating the experiment with a well-characterized Canadian chrysotile from the Cassiar Mine, British Columbia. This sample was heated in air in two stages, the

first, at 700°C, to completely oxidise the Fe^{2+} initially present, and the second, at 1200°C to ascertain whether the Fe^{2+} could be re-established. After heating at 1200°C, a strong Fe^{2+} spectrum was recorded, with parameters identical to those of the analogous Nelson sample. In addition, however, the Cassiar spectrum contained a weak 6-line magnetically split feature, which appears first in the sample heated at 700°C, and has Mössbauer parameters characteristic of haematite (Fe_2O_3). A second very weak 6-line spectrum can also be detected in this sample, with an internal field similar to magnetite (Fe_3O_4) or maghemite (γ-Fe_2O_3).

The possibility that the development of an Fe^{2+} spectrum may be an artifact of the furnace atmosphere or the heating procedure was investigated by heating a Nelson sample in an electric tube furnace, with both ends open to the air, rather than in the electric muffle furnace in which the elements are in direct contact with the (static) furnace atmosphere. The spectrum of the tube furnace sample was identical with those from the muffle furnace, but also contained a hint of a single six-line spectrum with characteristics more like maghemite than haematite. These results suggest, however, that the Fe^{2+} spectra are real and reproducible, and raise the interesting question of their formation mechanism.

A recent solid-state ^{29}Si and ^{25}Mg MAS NMR investigation of chrysotile decomposition [1] suggests that the mineral dehydroxylates in two steps, preceded by a degree of segregation into Mg-rich and Si-rich regions. The former regions dehydroxylate first, forming forsterite, from a short-lived Mg-rich dehydroxylate, designated dehydroxylate I. The Si-rich regions then form a dehydroxylate II, which has NMR characteristics of a layer-lattice structure, and decomposes to enstatite and free silica. The latter than progressively reacts with some of the forsterite initially formed, producing more enstatite, up to an equimolar ratio with forsterite. This proposed sequence is shown schematically in Fig. 7, which also includes the status of the iron throughout the various reaction stages, based on the following interpretation of the Mössbauer results, and the assumption that charge balance is maintained in the sample throughout the reaction.

The Mössbauer data for the unheated Nelson chrysotile indicate that of the 1.16% Fe present, 0.35% is Fe^{2+} and 0.81% is Fe^{3+}, of which 0.58% are in octahedral and 0.23% in tetrahedral sites. This corresponds to about 0.028 octahedral Fe^{3+} per unit cell and about 0.011 tetrahedral Fe^{3+} per unit cell, and a nett charge imbalance of 0.017 per unit cell. According to O'Hanley and Dyar [11], such a charge imbalance is compensated for by the presence of cation vacancies, which would amount in this case to 0.008 vacancies per unit cell. The substitution of 0.017 octahedral Fe^{2+} per unit cell for Mg gives rise to no additional charge imbalance in the unheated material.

Thermal reaction below the dehydroxylation temperature results in the oxidation of octahedral Fe^{2+} to Fe^{3+}, with a concomitant movement of tetrahedral Fe^{3+} into octahedral sites (Fig. 4), which contain approximately sufficient vacancies to accommodate the extra atoms. The movement of tetrahedral Fe^{3+} into octahedral vacancies will not change the overall charge balance, because every tetrahedral Fe^{3+}/octahedral vacancy combination is balanced by three octahedral Fe^{3+} substituents; the new configuration of four octahedral Fe^{3+}, each representing one

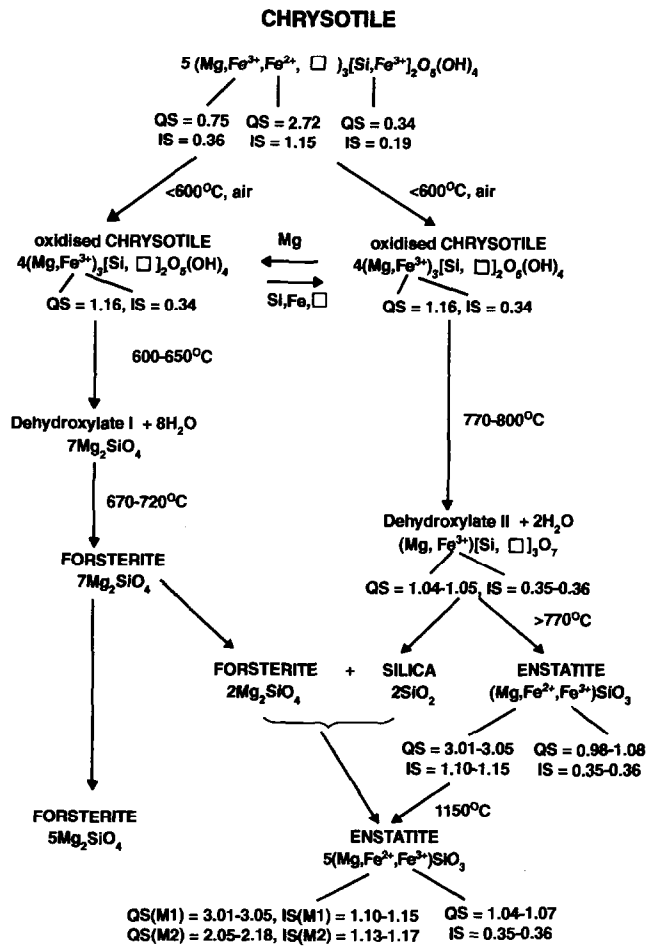

Fig. 7. Semi-schematic representation of the thermal sequence of chrysotile based on MAS NMR [1] and Mössbauer results. Isomer shifts quoted with respect to natural iron.

formal positive charge is balanced by the four formal negative charges on the new tetrahedral vacancy. However, the oxidation of octahedral Fe^{2+} to Fe^{3+} will increase the charge imbalance, and lead to a configuration which cannot be relieved by the removal of octahedral cations, because the total number of cations remains constant. Because this oxidation precedes the dehydroxylation, the mechanism must involve reaction with atmospheric oxygen at the fibre surfaces, with the formation of O^{2-}

$$2Fe^{2+} + \tfrac{1}{2}O_2 \rightarrow 2Fe^{3+} + O^{2-} \quad (1)$$

At this point, the sample still retains the XRD characteristics of chrysotile, but the Mössbauer data indicate that the octahedral Fe^{3+} sites are extremely distorted,

possibly due to the presence of the newly formed cation vacancies associated with the O^{2-}.

At about this stage (610°C), dehydroxylation is triggered, forming water by the reaction

$$2OH^- \rightarrow H_2O + O^{2-} \quad (2)$$

According to the recent MAS NMR studies [1], the phase assemblage immediately following initial dehydroxylation is forsterite and Si-rich regions which later form dehydroxylate II. Because the Fe^{3+} Mössbauer parameters of the sample at this stage are totally different to those reported for Fe^{3+} in forsterite [19], it may be inferred that the iron initially remains associated with dehydroxylate II, which by its nature will contain high concentrations of lattice defects. When these defects are annihilated by the transformation into enstatite ($MgSiO_3$), the Mössbauer results indicate the concomitant conversion of octahedral Fe^{3+} (in the sites designated B) into Fe^{2+} having typical enstatite Mössbauer parameters. Thus, the higher temperature valency change appears to be associated with the transformation of an Si-rich dehydroxylate, probably containing a high proportion of cation vacancies and O^{2-}, to enstatite and amorphous SiO_2. Because the number of cation sites per O^{2-} is smaller in both chrysotile and dehydroxylate II than in either forsterite or enstatite, conversion of the former to the latter involves the removal of the excess O^{2-} and defects which were introduced during the initial oxidation. By analogy with the reaction proposed for the removal of defects from the Si-rich phase from dehydroxylated kaolinite [23], one possible reaction sequence might be

$$\underset{\text{Dehydroxylate II}}{MgSi_3O_7 - 2\square^{(+)}} \rightarrow \underset{\text{Enstatite}}{MgSiO_3} + SiO_2 + SiO + O^{2-} \quad (3)$$

where $\square^{(+)}$ denotes a cation vacancy.

$$O^{2-} + 2Fe^{3+} \rightarrow \tfrac{1}{2}O_2 + 2Fe^{2+} \quad (4)$$

gives an overall reaction of

$$MgSi_3O_7 + 2Fe^{3+} - 2\square^{(+)} \rightarrow MgSiO_3 + 2Fe^{2+} + SiO + SiO_2 + \tfrac{1}{2}O_2 \quad (5)$$

Thus, the driving force for the elimination of vacancies is satisfied by the elimination of O^{2-} near the vacancy site as O_2, with charge neutrality being maintained by the reduction of Fe^{3+} to Fe^{2+}, effectively a reversal of the lower temperature oxidation.

The temperature at which the second Fe^{2+} doublet appears (>950°C) makes it unlikely that this is associated with forsterite, because by this stage in the reaction, the concentration of forsterite is being depleted by reaction with the excess SiO_2 to form more enstatite. Thus, the later appearance of this Mössbauer doublet may simply result from the improved resolution of the Fe^{2+} resonances as their concentration increases. However, this result implies that the enstatite formed from this chrysotile takes iron preferentially into the M1 sites, by contrast with the M2 site preference for iron reported by Lin et al. [20]. The reason for this discrepancy is not clear.

3.4. Practical implications of these results

It has been suggested [24] that the toxicity of fibrous blue asbestos (crocidolite, $Na_2(Fe^{2+},Mg)Fe_2^{3+}Si_8O_{22}(OH)_2$) can be lowered by treatment with ferric salts, which have been shown by Mössbauer spectroscopy to exchange preferentially on to surface sites and ferrous sites which do not normally contain Fe^{3+}. The rationale for converting blue asbestos to a ferric form arises from the fact that one mechanism by which the body protects itself from asbestosis is by coating the fibres with organic ferric oxides; this replacement of ferrous ions suppresses the formation in the body of hydroxyl free radicals by Fenton-type reactions [24]. However, such a mechanism does not appear to operate in chrysotile, in which the neurotoxicity, macrophage destruction and haemolytic activity are all reported to increase when the sample is heated at 600–800°C [25], the temperature shown by the present Mössbauer study to correspond to complete Fe^{2+} oxidation. The reported disappearance of toxicity in chrysotile heated to above 1000°C [25] is shown by the present work to correspond with the reappearance of Fe^{2+}, suggesting that by contrast with the more iron-rich asbestos minerals, the removal of harmful effects by thermal treatment of chrysotile may be more related to changes in physical properties (fibre embrittlement, dimensions, etc.) than to the valency of such iron as is present.

These results may also have interesting geochemical implications for the metamorphic formation of olivine and pyroxene from serpentines, especially chrysotile, because they suggest that even in surface intrusions, in the presence of air, predominantly ferrous phases seem to be preferred.

References

[1] K.J.D. MacKenzie and R.H. Meinhold, Am. Mineral., 79 (1994) 43.
[2] C. Blaauw, G. Stroink, W. Leiper and M. Zentilli, Can. Mineral., 17 (1979) 713.
[3] T.V. Malysheva, L.M. Satarova and N.P. Polyakova, Geochem. Int., 14 (1977) 117.
[4] W.J. Murphy and R.A. Ross, Clays Clay Miner., 25 (1977) 78.
[5] J. Khorami, D. Choquette, F.M. Kimmerle and P.K. Gallagher, Thermochim. Acta, 76 (1984) 87.
[6] M.C. Ball and H.F.W. Taylor, Mineral. Mag., 33 (1963) 467.
[7] G.W. Brindley and R. Hayami, Mineral. Mag., 35 (1965) 189.
[8] A.K. Datta, B.K. Samantaray and S. Bhattacherjee, Bull. Mater. Sci., 8 (1986) 497.
[9] H. DeSouza Santos and K. Yada, Clays Clay Miner., 27 (1979) 161.
[10] I. Rozenson, E.R. Bauminger and L. Heller-Kallai, Am. Mineral., 64 (1979) 893.
[11] D.S. O'Hanley and M.D. Dyar, Am. Mineral., 78 (1993) 391.
[12] M. Mellini, Am. Mineral., 67 (1982) 587.
[13] M. Mellini and P.F. Zanazzi, Am. Mineral., 72 (1987) 943.
[14] K.J.D. MacKenzie, M.E. Bowden and R.M. Berezowski, in G.J. Long and J.G. Stevens (Eds.), Industrial Applications of the Mössbauer Effect, Plenum, New York, 1986, p. 547.
[15] K.J.D. MacKenzie and R.M. Berezowski, Thermochim. Acta, 74 (1984) 291.
[16] K.J.D. MacKenzie, C.M. Cardile and I.W.M. Brown, Thermochim. Acta, 136 (1988) 247.
[17] K.J.D. MacKenzie, I.W.M. Brown, C.M. Cardile and R.H. Meinhold, J. Mater. Sci., 22 (1987) 2645.

[18] I.W.M. Brown, K.J.D. MacKenzie and R.H. Meinhold, J. Mater. Sci., 22 (1987) 3265.
[19] I. Shinno, Phys. Chem. Mineral., 7 (1981) 91.
[20] C. Lin, L. Zhang and S.S. Hafner, Am. Mineral., 78 (1993) 8.
[21] T.V. Malysheva and A.V. Ukhanov, Geochem. Int., 13 (1976) 96.
[22] K.J.D. MacKenzie, Rev. High Temp. Mater., 5 (1983) 251.
[23] K.J.D. MacKenzie, J. Inorg. Nucl. Chem., 32 (1970) 3731.
[24] G.R. Hearne, H. Pollak, J.A. van Wyk and M. Gulumian, Hyperfine Interactions, 73 (1992) 377.
[25] H. Hayashi, K. Koshi and H. Sakabe, Proc. Int. Clay Conf., Tokyo, 1 (1969) 903 (Israel Univ. Press, Jerusalem, 1969).